An atlas of seven zebrafish hox cluster mutants provides insights into sub/neofunctionalization of vertebrate Hox clusters

Kazuya Yamada[1,‡], Akiteru Maeno[2,*,‡], Soh Araki[1], Morimichi Kikuchi[1], Masato Suzuki[1], Mizuki Ishizaka[1], Koumi Satoh[1], Kagari Akama[1], Yuki Kawabe[1], Kenya Suzuki[1], Daiki Kobayashi[1], Nanami Hamano[1] and Akinori Kawamura[1,§]

ABSTRACT

Vertebrate Hox clusters are comprised of multiple Hox genes that control morphology and developmental timing along multiple body axes. Although results of genetic analyses using Hox-knockout mice have been accumulating, genetic studies in other vertebrates have not been sufficient for functional comparisons of vertebrate Hox genes. In this study, we isolated all of the seven hox cluster loss-of-function alleles in zebrafish using the CRISPR-Cas9 system. Comprehensive analysis of the embryonic phenotype and X-ray micro-computed tomography scan analysis of adult fish revealed several species-specific functional contributions of homologous Hox clusters along the appendicular axis, whereas important shared general principles were also confirmed, as exemplified by serial anterior vertebral transformations along the main body axis, observed in fish for the first time. Our results provide insights into discrete sub/neofunctionalization of vertebrate Hox clusters after quadruplication of the ancient Hox cluster. This set of seven complete hox cluster loss-of-function alleles provide a formidable resource for future developmental genetic analysis of the Hox patterning system in zebrafish.

KEY WORDS: Hox genes, Zebrafish, Sub/neofunctionalization, X-ray CT scan, Vertebrate evolution

INTRODUCTION

In bilaterian animals, Hox genes encoding the homeodomain transcription factors specify the positional identity of cells along the body axis. As one of the characteristic features, Hox genes are arranged in a cluster (Hox cluster) in most cases. The clustering of Hox genes in the chromosome has functional relevance. The positional order of Hox genes in each cluster corresponds to spatially-organized expression with a distinct anterior limit of the expression domain. Through this combinatorial collinear expression, Hox genes instruct the development of distinct morphology dependent on the positional information along the body axis.

In the early lineage of vertebrate evolution, the Hox cluster underwent drastic changes in terms of quality and quantity

(Duboule, 2007). Two rounds of whole-genome duplication (WGD) quadrupled a single ancestral Hox cluster (Dehal and Boore, 2005). Subsequently in the teleost lineage, Hox clusters were further duplicated by additional WGD. At present, zebrafish possess seven hox clusters, following the loss of the *hoxdb* cluster (Amores et al., 1998; Woltering and Durston, 2006), and tetrapods such as mice and humans retain four Hox clusters. Concomitant with the amplification of the Hox cluster number, the structure of vertebrate Hox clusters has been drastically changed to an organized and constrained structure (Duboule, 2007). For example, non-Hox genes are absent within the vertebrate Hox clusters, and the transcription of all Hox genes in each cluster is oriented from the same strand (Darbellay et al., 2019). The genomic size of the vertebrate Hox clusters is highly compacted compared with that of the invertebrate counterparts, partially by the elimination of repetitive DNA sequences. It has been proposed that these drastic changes in vertebrate Hox clusters contribute to the rapid vertebrate-specific morphological innovation (Duboule, 2007; Wagner et al., 2003).

Genetic studies using knockout mice have significantly expanded our understanding of the function of Hox genes in the vertebrate body plan. Several lines of evidence indicate that Hox genes play important roles in the specification of positional identity in vertebrate-specific morphologies such as the vertebral column (Fromental-Ramain et al., 1996; Horan et al., 1995; McIntyre et al., 2007; Wellik and Capecchi, 2003), limbs (Kmita et al., 2005; Zakany and Duboule, 2007) and internal organs such as the kidney (Wellik et al., 2002). However, it remains to be elucidated whether the roles of Hox genes that have been revealed by a number of studies in mice are conserved among vertebrates. From an evolutionary point of view, fish are distantly related to mice among vertebrates. Thus, zebrafish offer a plausible opportunity to elucidate the functional comparisons of vertebrate Hox genes. Indeed, functional conservation of homologous *HoxA/D* genes has been shown in the development of forelimbs in mice and the homologous pectoral fins in zebrafish (Kmita et al., 2005; Nakamura et al., 2016). On the other hand, functional discrepancies of Hox genes between mice and zebrafish such as hindbrain patterning and pharyngeal arch formation have been pointed out (McClintock et al., 2001, 2002). Thus, whether the functional roles of Hox genes are conserved or different among vertebrates at the levels of whole Hox clusters remains to be determined. Functional studies have so far been restricted to a small number of hox genes among the 48 hox genes in zebrafish (Breau et al., 2013; Hunter and Prince, 2002; McClintock et al., 2001, 2002; Nakamura et al., 2016; Waxman et al., 2008; Weicksel et al., 2014; Ye and Kimelman, 2020). A large number of zebrafish hox genes makes comprehensive comparisons with homologous mouse Hox genes difficult. Instead, the existence of four well-characterized Hox cluster-deleted knockout mice (for the murine *HoxB* cluster, *Hoxb1-Hoxb9* except *Hoxb13* are deleted) (Kmita et al., 2005; Medina-Martinez et al., 2000; Spitz et al., 2001;

[1]Division of Life Science, Graduate School of Science and Engineering, Saitama University, Shimo-okubo 255, Sakura-ku, Saitama 338-8570, Japan. [2]Plant Resource Development, Division of Genetic Resource Center, National Institute of Genetics, Yata 1111, Mishima, Shizuoka 411-8540, Japan.
*Present address: Cell Architecture Laboratory, National Institute of Genetics, Yata 1111, Mishima, Shizuoka 411-8540, Japan.
‡These authors contributed equally to this work

§Author for correspondence (akawamur@mail.saitama-u.ac.jp)

A.M., 0000-0003-0235-3478; A.K., 0000-0002-5618-7113

Suemori and Noguchi, 2000) prompted us to compare the functional roles of homologous Hox clusters between mice and zebrafish by generating hox cluster mutants in zebrafish. In this study, by using the CRISPR-Cas9 system, we isolated all of the seven individual hox cluster deficiencies in zebrafish. We examined the phenotypes of the seven hox cluster mutants during embryogenesis such as hindbrain patterning, jaw cartilage formation, pectoral fins and lateral line system. For adult fish of the five viable hox cluster homozygous mutants, the whole-body skeletons and soft tissues were analyzed by X-ray computed tomography (CT) scans. Although functional conservations between homologous Hox clusters were present in some cases, functional discrepancies of homologous Hox clusters between mice and zebrafish were widely observed. As zebrafish and mice share common ancestors that possessed four Hox clusters, our results suggest different subfunctionalization and neofunctionalization of vertebrate Hox clusters after the second round of WGD.

RESULTS

Isolation of each of the hox cluster loss-of-function alleles in zebrafish

Vertebrate Hox clusters generally do not contain non-Hox genes (Duboule, 2007). In the genome database, we confirmed that the seven hox clusters in zebrafish also do not possess non-hox genes (Fig. 1A). To elucidate the function of each hox cluster in zebrafish development, we tried to delete the corresponding genomic regions using the CRISPR-Cas9 system. We employed crRNA;tracrRNA duplex guideRNA (dgRNA), which was recently shown to be highly effective for introducing a genomic deletion in zebrafish (Hoshijima et al., 2019). For the generation of six hox cluster-deleted mutants (all of the clusters except for *hoxcb*), we used two dgRNAs that are targeted to both ends of hox genes in each cluster

(Fig. 1B). As a representative, the isolation of *hoxaa* cluster mutants is shown in Fig. 1C-F. Two dgRNAs specific to the exons of *hoxa1a* and *hoxa13a* were injected with Cas9 protein into fertilized embryos (Fig. 1C). Among the F1 offspring of the injected embryos, we identified fish with deletion of the genomic region corresponding to the *hoxaa* cluster (Fig. 1D). We also verified that the introduced genomic deletion resulted in a frameshift mutation so that an aberrant fusion protein was not produced. Furthermore, we confirmed that the targeted genomic region of the *hoxaa* cluster was specifically deleted in homozygous mutants (Fig. 1E,F), as transposition of the targeted genomic region was sometimes detected in the course of the generation of mutants. Likewise, the other five hox cluster mutants (*hoxab*, *hoxba*, *hoxbb*, *hoxca* and *hoxda*) were isolated and confirmed (Figs S1-S4,S6). As we could not isolate the *hoxcb* cluster-deleted mutant owing to technical difficulties, we instead introduced frameshift mutations in all of the four *hoxcb* genes in the same allele (Fig. S5). Taken together, we successfully isolated all of the seven individual hox cluster deficiencies in zebrafish.

Characterization of seven individual zebrafish hox cluster deficiencies during embryogenesis

Using these seven zebrafish hox cluster deficiencies, we carried out phenotype analysis during embryogenesis, in which vertebrate Hox genes have been shown to play essential roles. Hox genes have been shown to play crucial roles in the patterning of the hindbrain in vertebrate embryos (Trainor and Krumlauf, 2000), and segmental expression patterns of zebrafish hox genes, which are located in different hox clusters such as *hoxab*, *hoxba* and *hoxda*, in the rhombomeres have been characterized in detail (Prince et al., 1998b). To examine the role of each hox cluster in hindbrain patterning, we performed immunostaining for reticulospinal interneurons, which exhibit rhombomere-specific cell body shapes
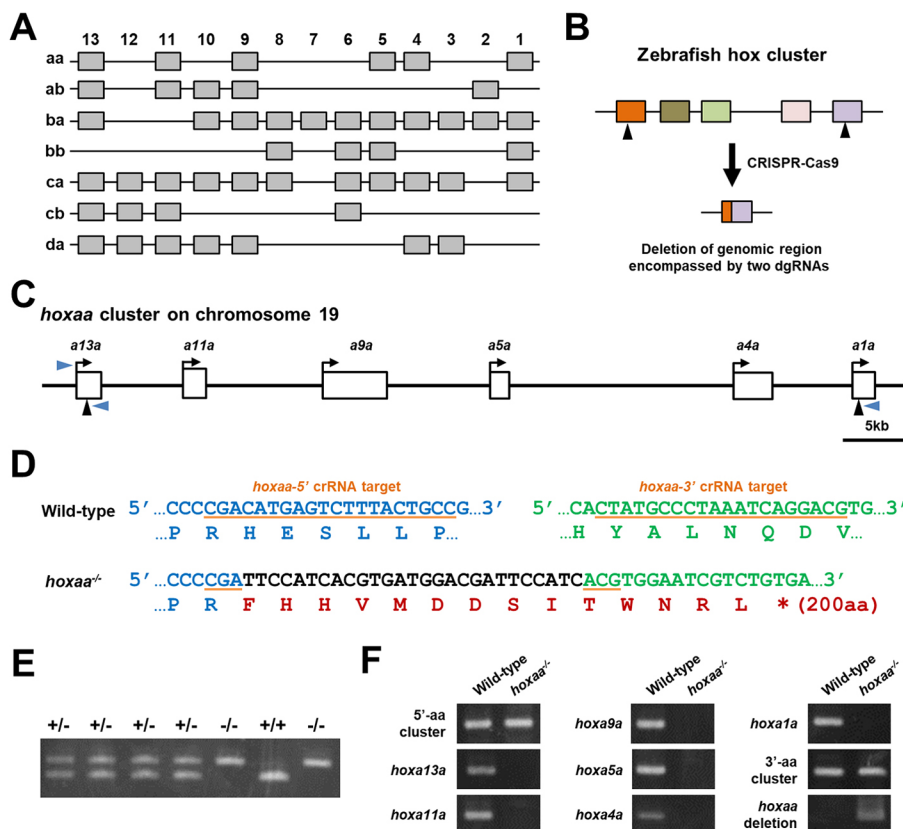
Fig. 1. Zebrafish hox clusters and isolation of *hoxaa* cluster-deleted mutants. (A) The zebrafish possesses 48 hox genes in seven hox clusters. (B) Strategy for deletion of the genomic region corresponding to the hox cluster. Two dgRNAs (arrowheads), which recognize hox genes located at both ends of hox clusters, were used to delete the target genomic region. (C) Schematic of the *hoxaa* cluster locus. Six hox genes in the *hoxaa* cluster are depicted as white rectangles. The arrow shows the orientation of the transcription of each hox gene. Two black arrowheads indicate the genomic loci of the target sequence of dgRNAs, which were used to delete the genomic region of the *hoxaa* cluster. (D) Large genomic deletion in the *hoxaa* cluster mutant. The flanking sequences of two dgRNAs-target are shown. The target sequence of *hoxaa*-5′ dgRNA is exon 1 of *hoxa13a* (blue letters), and *hoxaa*-3′ dgRNA is targeted to exon 1 of *hoxa1a* (green letters). The *hoxaa* mutant possessing a ∼56.4 kb deletion and a 27 bp insertion (black letters) was isolated. This indel mutation resulted in frameshift of *hoxa13a*. (E) PCR-based genotyping of embryos obtained by intercross between *hoxaa*$^{+/-}$ fish. Genotyping was carried out with the three primers shown by blue arrowheads in C. The sequences of primers and PCR cycles are shown in Table S3. (F) Specific deletion of the *hoxaa* cluster was confirmed by PCR. The genomic DNA extracted from wild-type and *hoxaa*$^{-/-}$ embryos was used as a template for PCR. The sequences of the primers used in this analysis are listed in Table S4.

2
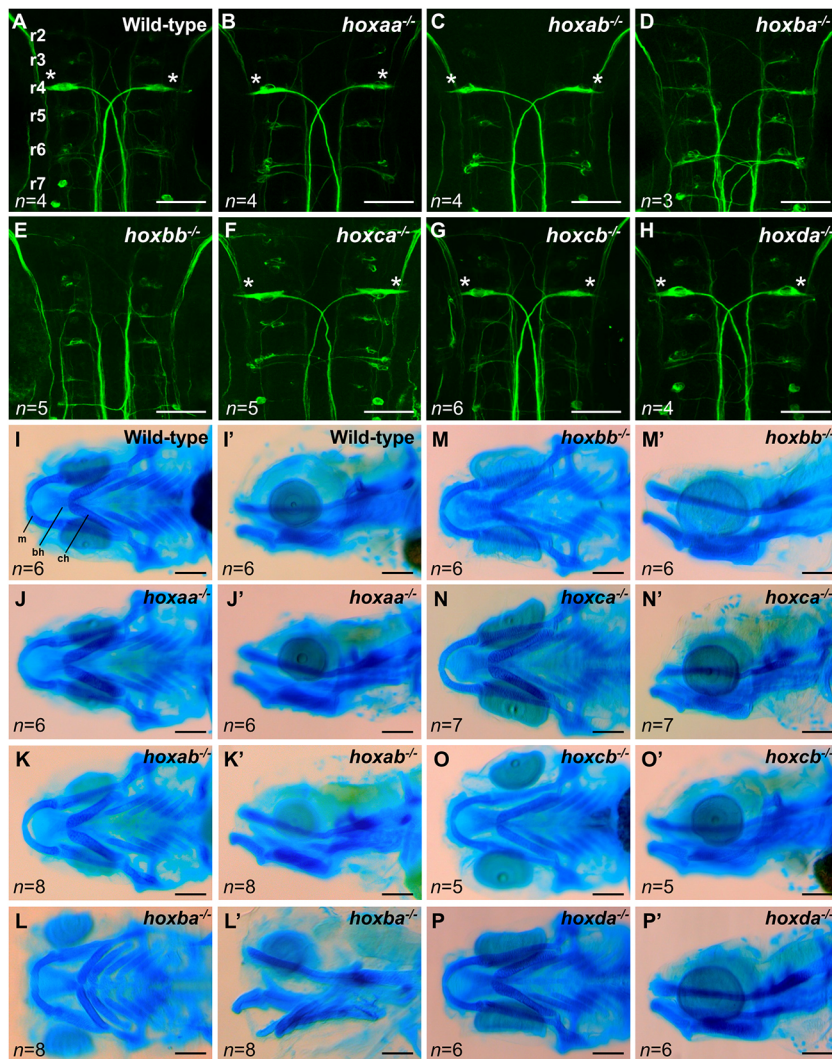
Fig. 2. Reticulospinal neurons and craniofacial cartilage in zebrafish hox cluster mutants. (A-H) Reticulospinal neurons in the hindbrain at 48 hpf were visualized by whole-mount immunostaining using anti-neurofilament RMO-44 antibody. Dorsal view of flat-mounted specimens after removal of the yolk. Mauthner cells located at r4 are indicated by asterisks. Hemizygous mutants for each hox cluster appeared indistinguishable from the wild-type. (I-P′) Craniofacial cartilages of zebrafish larvae at 5 dpf were stained with Alcian Blue. I-P show ventral view and I′-P′ show lateral view. bh, basihyal; ch, ceratohyal; m, Meckel's cartilage. Scale bars, 50 μm (A-H); 100 μm (I-P).

and axonal projection patterns (Metcalfe et al., 1986). In wild-type embryos at 48 hours post fertilization (hpf), contralaterally projecting r4-specific Mauthner neurons were evident on both sides (asterisks in Fig. 2A). In contrast, in *hoxba* and *hoxbb* cluster mutants, Mauthner neurons were rarely detected, but instead smaller projecting neurons were observed (Fig. 2D,E). The hindbrain defects observed in *hoxba* and *hoxbb* cluster mutants show significant similarity to the individual loss-of-function phenotypes of zebrafish *hoxb1a* and *hoxb1b*, respectively (McClintock et al., 2002; Weicksel et al., 2014), suggesting that other *hoxba* genes (such as *hoxb2a*, *hoxb3a* and *hoxb4a*, which are segmentally expressed in rhombomeres; Prince et al., 1998b) or *hoxbb* genes other than *hoxb1b* do not significantly contribute to the hindbrain patterning in zebrafish. In addition, no apparent morphological abnormality in reticulospinal neurons was observed in other hox cluster deficiencies (Fig. 2B,C,F-H).

Cranial neural crest cells derived from the hindbrain migrate to form pharyngeal arches that give rise to most of the cartilage and bone in the developing head (Minoux and Rijli, 2010). In mice, Hox genes have been shown to establish the positional identity of cranial neural crest-derived cells in pharyngeal arches (Trainor and Krumlauf, 2001). Thus, we characterized the contributions of each hox cluster to the formation of craniofacial cartilage in zebrafish (Fig. 2I-P). At 5 days post fertilization (dpf), we found

that abnormal morphology is evident only in *hoxba* cluster mutants. In *hoxba* cluster mutants, cartilages consisting of the basihyal and ceratohyal, which are derived from the second pharyngeal arch, were misshapen, and the connection between the basihyal and Meckel's cartilage was improper (Fig. 2L,L′). In addition, we observed that some *hoxba* cluster-deficient embryos at 7 dpf lacked the basihyal (Fig. S7). In zebrafish, knockdown of *hoxb2a* alone does not result in any defects in the pharyngeal arch, whereas simultaneous knockdown of *hoxa2b* and *hoxb2a* leads to major defects in the second pharyngeal arch (Hunter and Prince, 2002). As *hoxba* genes such as *hoxb2a*, *hoxb3a*, *hoxb4a* and *hoxb5a* are specifically expressed in the pharyngeal arches in zebrafish (Miller et al., 2004), abnormal morphology of pharyngeal arches in *hoxba* cluster mutants suggests that other *hoxba* genes cooperate with *hoxb2a* in the proper formation of pharyngeal arches. Despite severe defects in hindbrain patterning in *hoxbb* cluster mutants, craniofacial cartilage appeared to be unaffected (Fig. 2M,M′).

It is well known that Hox genes in *HoxA* and *HoxD* clusters regulate the proximal-distal patterning of developing limbs in mice (Kmita et al., 2005; Zakany and Duboule, 2007). The formation of the pectoral fin, which is a teleost homolog of the forelimb, is also regulated by the combinatorial expression of hox genes in zebrafish (Ahn and Ho, 2008; Nakamura et al., 2016; Sordino et al., 1995). To investigate the role of each hox cluster in the paired pectoral fin

DEVELOPMENT

3
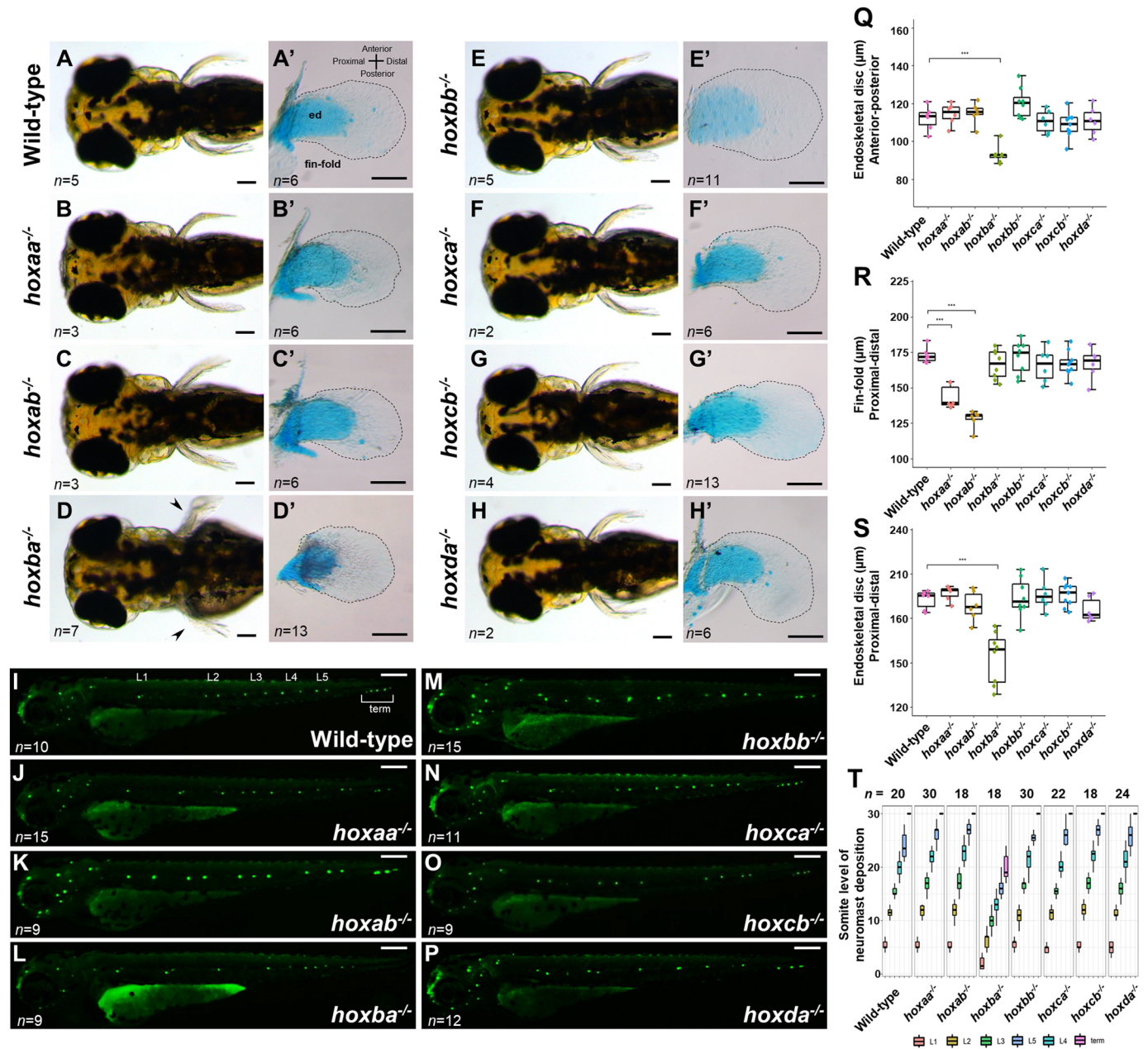
Fig. 3. Pectoral fins and lateral line neuromasts in zebrafish hox cluster mutants. (A-H) Pectoral fins of live hox cluster mutants at 3 dpf. Dorsal view. Arrowheads in D indicate pectoral fin malformation in *hoxba* cluster mutants. (A′-H′) Dissected pectoral fins at 5 dpf. Alcian Blue staining was performed to show cartilage cells (endoskeletal disc; ed). Hemizygous mutants for each hox cluster appeared indistinguishable from the wild-type. The margin of the fin-fold is emphasized by a dashed line. (I-P) Neuromasts in lateral lines were visualized in hox cluster mutants at 3 dpf. Posterior lateral line neuromasts are indicated from anterior-to-posterior as L1, L2, L3, L4, L5, and terminal (term) neuromasts. Hemizygous mutants for each hox cluster appeared indistinguishable from the wild-type. (Q) Comparison of the lengths of the endoskeletal disc along the anterior-posterior axis at the center of the fin. (R) Comparison of fin-fold lengths along the proximodistal axis in hox cluster mutants. (S) Comparison of the lengths of the endoskeletal disc along the proximodistal axis at the center of the fin. Box plot percentiles are: line, median; box, 25th and 75th percentiles; whiskers, 0th-25th and 75th-100th percentiles. The error bar represents the standard error. ***$P<0.001$ (two-tailed Student's *t*-test). (T) Positions of posterior lateral line neuromasts, which are located relative to the somite number, are compared in hox cluster mutants. Neuromasts located on both sides of the larvae were examined. Scale bars: 50 μm (A-H,I-P); 100 μm (A′-H′).

development, we examined the phenotype of homozygous embryos. In wild-type zebrafish, pectoral fins were present on both sides of larvae at 3 dpf (Fig. 3A). In contrast, *hoxba* cluster mutants apparently exhibited misshapen pectoral fins (Fig. 3D). At this stage, morphological abnormalities were not detectable in other hox cluster mutants including *hoxaa*, *hoxab* or *hoxda* cluster mutants (Fig. 3B,C,E-H). To examine the pectoral fin growth in more detail, we compared the lengths of the endoskeletal disc (cartilage) and

fin-fold. Using cartilage-stained pectoral fins at 5 dpf, we found that the endoskeletal disc in *hoxba* cluster mutants was shortened, whereas those in the other hox cluster mutants appeared normal (Fig. 3A′-H′,Q,S). On the other hand, the length of the fin-fold along the proximal-distal axis was decreased in *hoxaa* and *hoxab* cluster mutants (Fig. 3A′-C′,R). The differences in phenotypes between *hoxba* and *hoxaa/ab* cluster mutants suggest their different functional roles in pectoral fin development. The other hox cluster mutants did

DEVELOPMENT

not exhibit significant abnormal lengths of the fin-fold (Fig. 3R). Despite the specific expression of *hoxc6a* and *hoxda* genes in pectoral fin buds (Ahn and Ho, 2008; Nakamura et al., 2016; Neumann et al., 1999; Sordino et al., 1995), apparent abnormalities of pectoral fin development were not observed in *hoxca* or *hoxda* cluster mutants.

We also investigated the lateral lines that comprise a number of individual sensory organs, called neuromasts. In the posterior lateral line, collective migration of primordial cells from anterior to posterior results in the deposition of several groups of neuromasts at regular intervals on the surface of larvae (Ledent, 2002) (Fig. 3I). In zebrafish, *hoxb8a* was shown to control this cell migration (Breau et al., 2013). As in the case of *hoxb8a* knockdown embryos, neuromasts in *hoxba* cluster mutants were located more anteriorly than those in wild-type zebrafish (Fig. 3L,T). The number of neuromasts was not affected in *hoxba* cluster mutants (Fig. S8), suggesting retarded cell migration. Although several hox genes are expressed in the migrating lateral line primordial cells (Thisse et al., 2001), the deposition of posterior lateral line neuromasts in other hox cluster mutants appeared to be normal (Fig. 3J,K,M-P,T).

Viability of zebrafish hox cluster-deficient fish

We proceeded to investigate the roles of each hox cluster in later development. By intercross between each hox cluster-deficient hemizygous fish, the offspring were raised to examine whether homozygous mutants are viable or lethal. Among intercrossed juvenile fish at ∼1-2 months of age, *hoxab* cluster-deleted and *hoxba* cluster-deleted homozygous mutants were not identified (Table 1), indicating that deletion of the *hoxab* or *hoxba* cluster causes lethality. The *hoxba* cluster mutants exhibited a severe expansion of the pericardial cavity in addition to the several defects described above. The *hoxab* cluster mutants showed a relatively mild abnormality, such as slightly short pectoral fins during embryogenesis; however, we could not identify viable *hoxab* cluster homozygous fish. In contrast, homozygous fish deficient in the other five hox clusters (*hoxaa*, *hoxbb*, *hoxca*, *hoxcb* and *hoxda*) survived to adulthood, although the survival rate of homozygous mutants was lower than that of siblings (Table 1).

Table 1. Survival rate of seven hox cluster mutants

Genotype of the parents	*n*	+/+	+/−	−/−	Survival rate
hoxaa^{+/−}× *hoxaa*^{+/−}	97	34 (35.1%)	52 (53.6%)	11 (11.3%)	45.2%
hoxab^{+/−}× *hoxab*^{+/−}	102	47 (46.1%)	55 (53.9%)	0 (0.0%)	0.0%
hoxba^{+/−}× *hoxba*^{+/−}	71	41 (57.7%)	30 (42.2%)	0 (0.0%)	0.0%
hoxbb^{+/−}× *hoxbb*^{+/−}	59	22 (37.3%)	35 (59.3%)	2 (3.4%)	13.6%
hoxca^{+/−}× *hoxca*^{+/−}	103	28 (27.2%)	72 (69.9%)	3 (2.9%)	11.7%
hoxcb^{+/−}× *hoxcb*^{+/−}	54	16 (29.6%)	28 (51.9%)	10 (18.5%)	72.6%
hoxda^{+/−}× *hoxda*^{+/−}	116	41 (35.3%)	68 (58.6%)	7 (6.0%)	24.1%

Header spanning note: "Genotype of the offspring juvenile fish" spans the +/+, +/− and −/− columns.

Embryos were obtained by natural spawning of several intercrosses between each of the hox cluster hemizygous mutants and raised to juvenile fish of ∼1 to 2 months of age. Then PCR-based genotyping was carried out to determine the genotypes of offspring. The survival rate of homozygous mutants was calculated by dividing the percentage of identified homozygous mutants by 25% expected from Mendel's law.

X-ray micro-CT scan analysis for five viable hox cluster mutants

Using these viable homozygous mutants, we performed X-ray micro-CT scan analysis to investigate the whole-body skeletons in detail. As is often observed in Hox knockout mice (Fromental-Ramain et al., 1996; Horan et al., 1995; McIntyre et al., 2007; Wellik and Capecchi, 2003), anterior homeotic transformation of the vertebral column was observed in zebrafish hox cluster mutant fish (Fig. 4; Movies 1-10). The Weberian apparatus, which consists of four ossicles to transmit the vibration of the swim bladder to the inner ear, is a specialized structure in the anteriormost region of the vertebral column in fish of the Ostariophysian, including zebrafish (Grande and Young, 2004; Sanger and McCune, 2002). In wild-type zebrafish, the tripus, which exhibits a fan-shaped bone of the Weberian apparatus, was located on both sides of the 3rd vertebra (Fig. 4A-C). In contrast, such a unique structure of the tripus was severely misshaped and turned out to be laterally-extending bone in *hoxca* cluster mutants (Fig. 4J-L). In addition, the altered bone in *hoxca* cluster mutants was attached to the anterior portion of the 3rd vertebra, whereas the tripus was attached to the center of the 3rd vertebra in wild-type zebrafish. These abnormal morphologies resemble the lateral process, which is laterally extending bone attached to the anterior portion of the 2nd vertebra, suggesting anterior homeotic transformation in the Weberian apparatus in *hoxca*^{−/−} fish. Besides, the os suspensorium, which is ventrally extending bone from the 4th vertebra, was found to be completely missing in *hoxca* cluster mutants, although the transverse process of vertebra 4 (tp4), which also extends lateral-ventrally from the 4th vertebra, was formed (Fig. 4J-L). Furthermore, *hoxcb* cluster mutants exhibited a slight morphological abnormality of shortening of the anterior portion of the tripus (asterisks in Fig. 4M,N). In *hoxbb* cluster mutants, the width of the tripus was slightly shortened, although the patterning of the tripus appeared normal (Fig. 4G-I). The other viable hox cluster mutants (*hoxaa* and *hoxda*) showed indistinguishable morphology of the Weberian apparatus in comparison with that of wild-type zebrafish (Fig. 4A-F,P-R).

In addition, anterior homeotic transformation was detected in the pleural-to-caudal transition regions of the vertebral column in hox cluster mutants (Fig. 4S-X). Although the identity of the vertebral column has been reported to vary in zebrafish (Bird and Mabee, 2003), our wild-type zebrafish generally possessed nine pairs of pleural ribs on the 5th-13th vertebrae and short ventrally extending bones from the 14th vertebra (Fig. 4S; Table S1). In contrast, *hoxaa*, *hoxca* and *hoxda* cluster mutants exhibited long pleural ribs from the 14th vertebra (Fig. 4T,V,X; Table S1), which show similarities to the 13th vertebra. In wild-type zebrafish, the ventrally extending bone (hemal arch) from the 15th vertebra reached the dorsal tip of the first radial attached to the anal fin (Fig. 4S; Table S1). However, in *hoxca* and *hoxda* cluster mutants, the 15th vertebra exhibited morphology similar to that of the 14th vertebra in wild-type zebrafish, and the 16th vertebra of the mutants resembled the 15th vertebra of wild-type zebrafish (Fig. 4V,X; Table S1). On the other hand, *hoxbb* and *hoxcb* cluster mutants did not show such anterior transformation (Fig. 4U,W; Table S1). These results provide the first genetic evidence that anterior transformation of the vertebral column indeed occurs in zebrafish hox cluster mutants.

We also found that the number of vertebrae was increased in hox cluster mutants. Our wild-type zebrafish usually possessed 31-33 vertebrae in total (Fig. 5A,O). However, *hoxca* cluster mutants exhibited an increased number of vertebrae, 34-37, although the other four viable hox cluster mutants did not exhibit noticeable differences (Fig. 5A-F,O). As the number of somites is linked to the
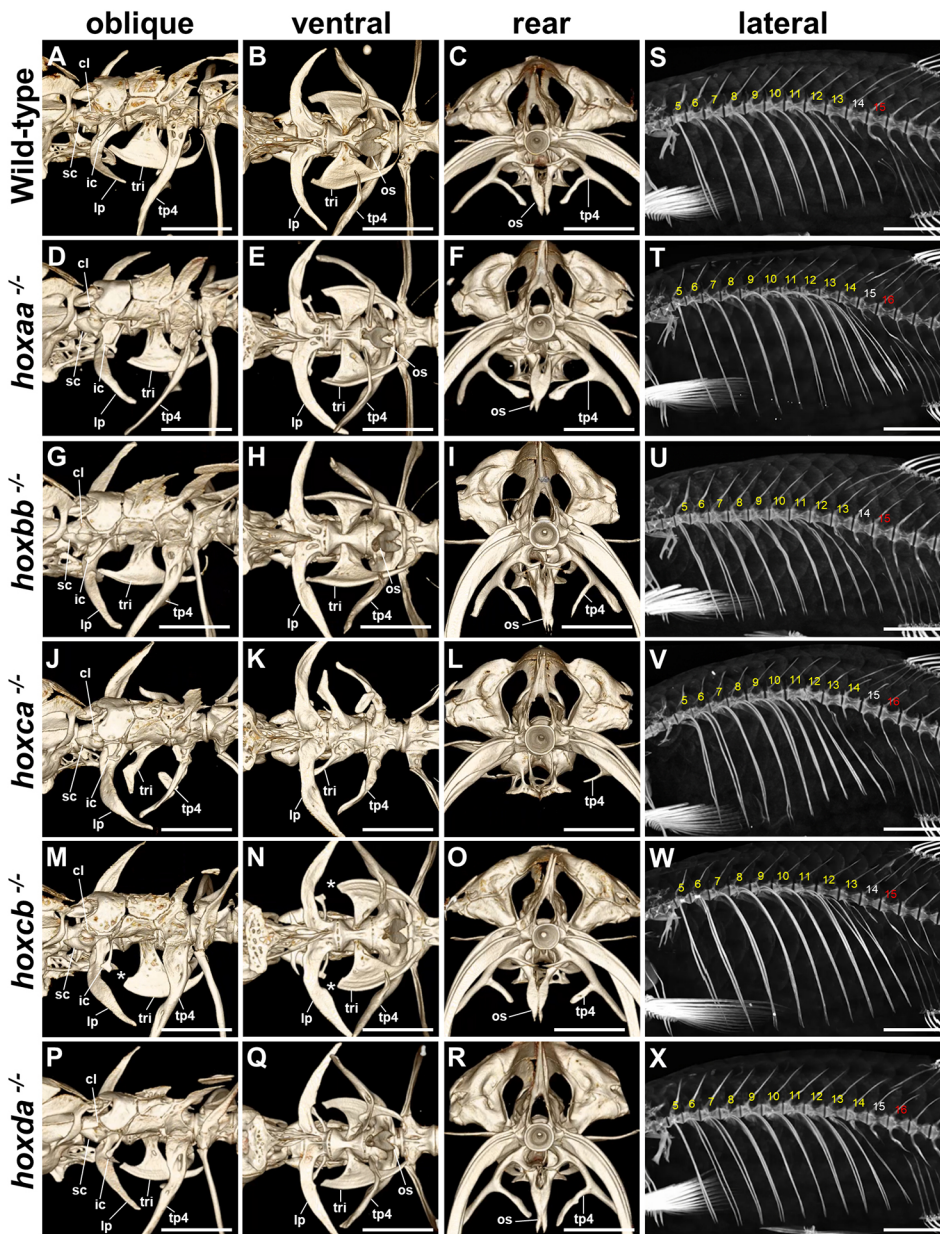
Fig. 4. Anterior homeotic transformation of the Weberian apparatus and pleural-to-caudal vertebrae in hox cluster mutants. (A-R) The anteriormost vertebrae including the Weberian apparatus in wild-type zebrafish and hox cluster mutants were examined by micro-CT scanning and are shown as 3D-VR images. The Weberian apparatus is composed of the four ossicles including the tripus (tri), intercalarium (ic), scaphium (sc) and claustrum (cl), in the anteriormost vertebrae. Other ossicles such as the os suspensorium (os), transverse process of vertebra 4 (tp4) and lateral process (lp) are indicated in the panels. (S-X) Pleural ribs in wild-type and hox cluster mutants (n=7 for wild-type; n=4 for $hoxaa^{-/-}$; n=2 for $hoxbb^{-/-}$; n=3 for $hoxca^{-/-}$; n=4 for $hoxcb^{-/-}$; n=2 for $hoxda^{-/-}$) were subjected to micro-CT scan analysis, and representative images are shown. The number represents the position of a vertebra from the first vertebra. The yellow number indicates the vertebra possessing the pleural ribs. The white number indicates the vertebra possessing the short ribs. The red number indicates the vertebra possessing the hemal arch that extends to the anteriormost radial in the anal-fin ray. In Table S1, the vertebral phenotypes are summarized and two $hoxca^{-/-}$ fish stained with Alizarin Red were included. $hoxbb^{-/-}$ and $hoxda^{-/-}$ are male and wild-type, $hoxaa^{-/-}$, $hoxca^{-/-}$ and $hoxcb^{-/-}$ are female. Movies 1-10 show micro-CT scans. Scale bars: 1 mm (A-R); 2 mm (S-X).

number of vertebrae (Morin-Kensicki et al., 2002), we visualized the somite boundaries of all hox cluster mutants at 2 dpf (Fig. 5G-N). Consistent with the increased number of vertebrae, we found that the number of somite boundaries was increased in *hoxca* cluster mutants (Fig. 5L,P). An increase of the body length along the anterior-posterior axis in *hoxca* cluster mutants was not detected, mainly due to the slight increase of small somites. Among the other hox cluster mutants, *hoxab* cluster mutants also exhibited an increase of somite number (Fig. 5I,P). Although *hoxab* cluster mutants were not viable (Table 1), these results suggest that the *hoxab* cluster, as well as the *hoxca* cluster, contributes to the regulation of somite/vertebra number in zebrafish. Furthermore, we also confirmed that the position of the pelvic fins along the anterior-posterior axis was not significantly affected in the five viable hox cluster-deficient mutants (Fig. S9).

Finally, we examined the whole-body tissues of surviving hox cluster mutant fish using X-ray micro-CT scans (Fig. 6; Movies 11-20). In wild-type zebrafish, anterior and posterior swim bladder lobes are present in the abdomen of adult zebrafish (Parichy et al., 2009) (Fig. 6A). However, we found that *hoxca* cluster mutant fish possessed a single swim bladder lobe (Fig. 6D). This morphological abnormality was specifically evident in *hoxca* cluster mutants, and apparent morphological defects in the swim bladder and other tissues were not observed in other hox cluster mutants (Fig. 6A-F).

DISCUSSION

In this study, we isolated loss-of-function alleles for all of the seven hox clusters in zebrafish. Using hox cluster mutants, we performed not only embryonic phenotype analysis but also X-ray micro-CT scan analysis for the whole-body skeletons and tissues in viable homozygous fish. In mice, four individual Hox cluster-deleted mutants have been generated and characterized in detail (Kmita et al., 2005; Medina-Martinez et al., 2000; Minoux et al., 2009; Soshnikova et al., 2013; Spitz et al., 2001; Suemori and Noguchi, 2000; Vieux-Rochas et al., 2013). Hereafter, we discuss the
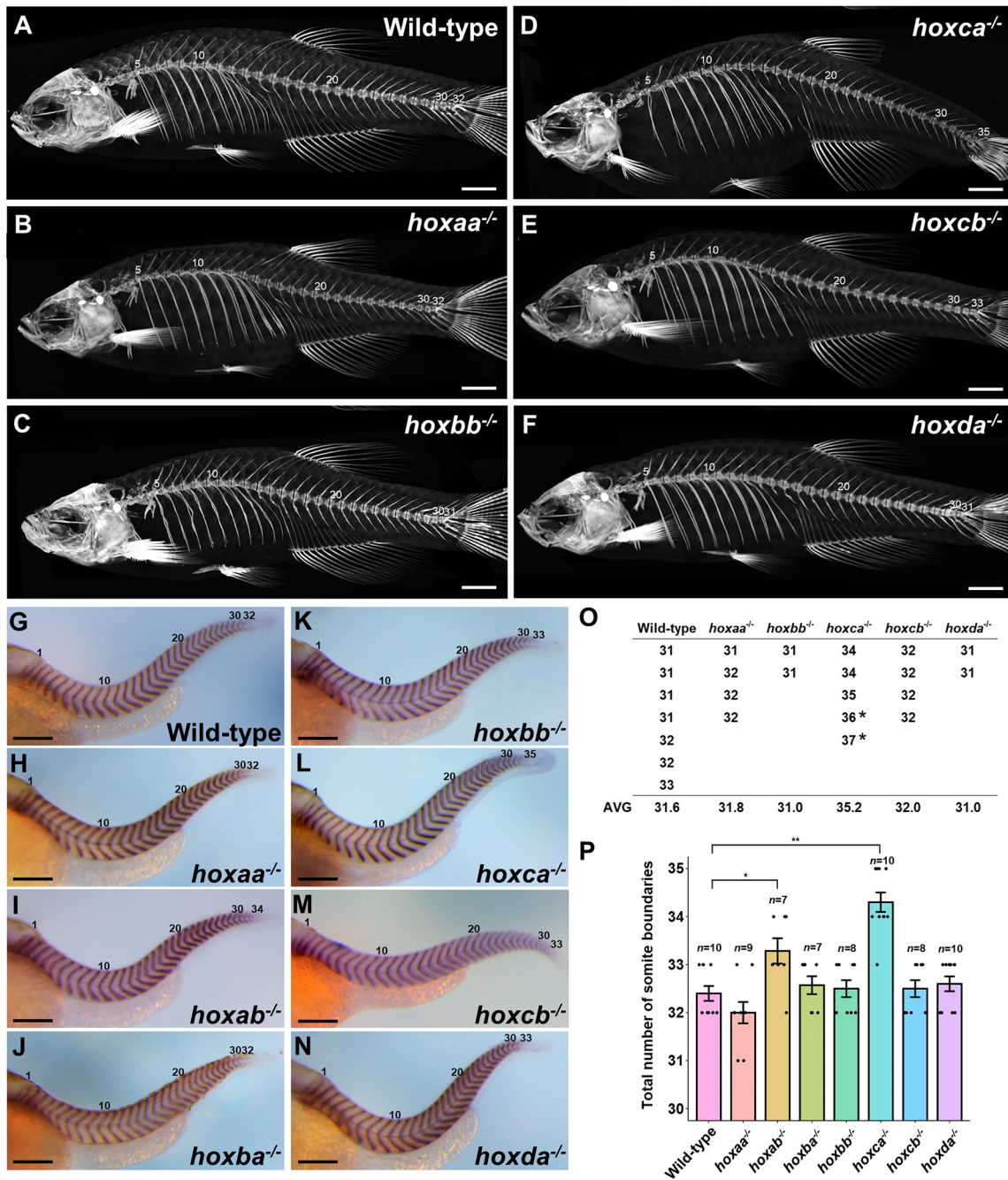
Fig. 5. Total numbers of vertebrae and somite boundaries in hox cluster mutants. (A-F) Whole-body skeletons were analyzed by micro-CT scanning. Adult fish (*n*=7 for wild-type; *n*=4 for *hoxaa*⁻/⁻; *n*=2 for *hoxbb*⁻/⁻; *n*=3 for *hoxca*⁻/⁻; *n*=4 for *hoxcb*⁻/⁻; *n*=2 for *hoxda*⁻/⁻) were examined by micro-CT scanning, and representative images are shown. (G-N) Expression patterns of the segment boundary marker, *xirp2a/cb1045*, in hox cluster homozygous embryos at 2 dpf. Lateral views. The number of somite boundaries from the anteriormost boundary is indicated. After staining, genotyping was performed. Hemizygous mutants for each hox cluster were indistinguishable from the wild-type. (O) Total numbers of vertebrae in hox cluster mutants. The numbers of vertebrates were counted using micro-CT scan images. In *hoxca* cluster mutants, two adult fish stained with Alizarin Red were included (indicated by the asterisk). (P) Comparison of the total numbers of somite boundaries in zebrafish hox cluster mutants. The numbers of somite boundaries in the mutants were compared by counting the segment boundaries stained with *xirp2a/cb1045*. Error bars represent the standard error. *P<0.05, **P<0.01 (two-tailed Student's *t*-test). Scale bars: 2 mm (A-F); 200 μm (G-N).

phenotypes of zebrafish hox cluster mutants in comparison with those of mouse Hox cluster mutants.

The present study revealed that *hoxba* cluster mutants show the most severe defects during embryogenesis among the seven hox cluster mutants in zebrafish. Several defects were observed in hindbrain patterning, jaw formation, pectoral fin formation and positioning of posterior lateral lines, although another *HoxB*-

derived *hoxbb* cluster is intact. These results suggest that the zebrafish *hoxba* cluster contains several hox genes which play crucial roles in the early embryogenesis. Besides, the zebrafish *hoxba* cluster is the only cluster that contains the paralogous group 7 (PG7), *hoxb7a* (Fig. 1A). Therefore, the deletion of the *hoxba* cluster results in complete lack of PG7 function, which cannot be compensated by other clusters. In contrast to zebrafish *hoxba* cluster

7
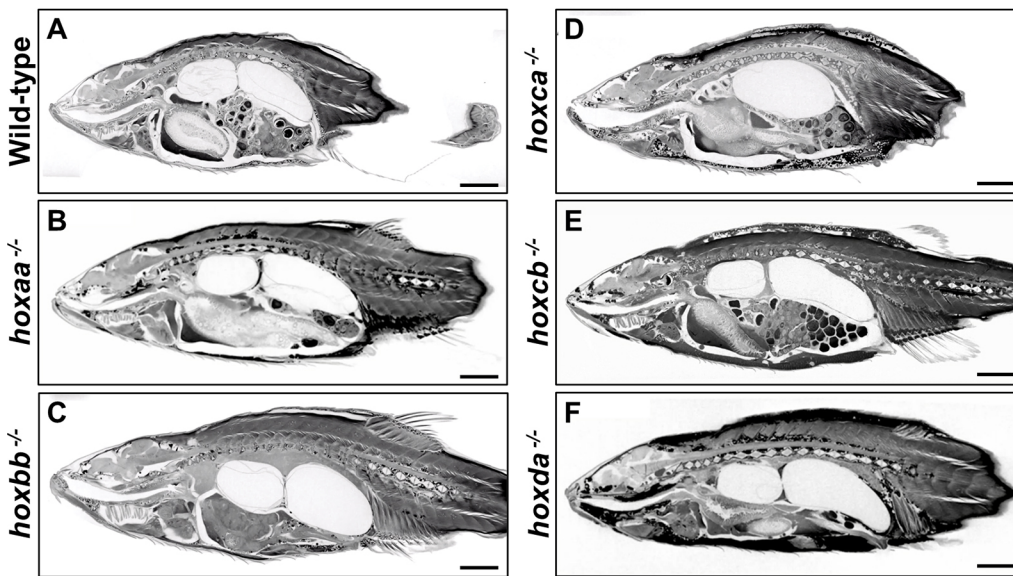
Fig. 6. Whole-body tissues of hox cluster mutants. (A-F) Whole-body tissues were analyzed by micro-CT scanning. After the micro-CT scanning for skeleton analysis, soft tissues of the same specimens were stained with Lugol's solution, and the stained tissues were subject to micro-CT scanning. Adult males (*hoxbb*$^{-/-}$ and *hoxda*$^{-/-}$) and females (wild-type, *hoxaa*$^{-/-}$, *hoxca*$^{-/-}$ and *hoxcb*$^{-/-}$) were used. Eggs are seen in the abdomen of female fish. Movies 11-20 show micro-CT scan 3D movies of transverse and sagittal sections. Scale bars: 2 mm.

mutants, *Hoxb1-Hoxb9*-deleted mutant mice exhibit only slight defects: anterior transformation along the cervical and thoracic vertebral column and some cranial nerve defects (Medina-Martinez et al., 2000). Although cranial nerve defects are commonly observed, morphological abnormalities in jaw and forelimbs have not been reported in *Hoxb1-Hoxb9*-deleted mutant mice (Medina-Martinez et al., 2000). In mice, morphological defects in the cranial facial skeleton are caused by deletion of the *HoxA* cluster (Minoux et al., 2009), although additional deletion of *Hoxb1-Hoxb9* enhances the phenotype of *HoxA* cluster mutants (Vieux-Rochas et al., 2013). On the other hand, knockout of mouse *Hoxb13* increases the number of tail vertebrae (Economides et al., 2003). However, in zebrafish *hoxba* and *hoxbb* cluster mutants, we did not detect any increase in the number of somite boundaries (Fig. 5P), which is associated with the number of vertebrae. It is unlikely that *hoxba* and *hoxbb* clusters redundantly control the number of somite boundaries because the *hox13* paralogous gene is only present in the *hoxba* cluster (Fig. 1A). Instead, such an increase is rather prominent in other hox cluster mutants such as *hoxca* and *hoxab* clusters, which possess *hoxc13a* and *hoxa13b*, respectively (Fig. 5P). These results suggest that the responsible Hox genes are not always located in homologous Hox clusters between zebrafish and mice, although the function of responsible Hox genes is conserved, suggesting different subfunctionalization of Hox clusters in vertebrate evolution.

HoxC cluster mutant mice do not show any drastic embryonic abnormalities but show a series of anterior transformations of the vertebral column (Suemori and Noguchi, 2000). Similarly, in zebrafish, *hoxca* and *hoxcb* cluster mutants do not show severe embryonic defects, but *hoxca* cluster mutants also show the anterior transformation of vertebral column (Fig. 4V). In *hoxca* cluster mutants, unique defects were observed in teleost-specific structures such as the Weberian apparatus and swim bladder (Figs 4J-L and 6D). The *hoxcb* cluster mutants also exhibit weak defects in the Weberian apparatus (Fig. 4M-O). As the anterior expression boundaries of *hoxc6a* and *hoxc6b* correspond to the 5th somite, which gives rise to the anterior vertebrae in zebrafish (Morin-Kensicki et al., 2002; Prince et al., 1998a), we presume that *hoxc6a* and *hoxc6b* are plausible candidate genes responsible for the defects in formation of the Weberian apparatus. In addition, zebrafish *hoxc4a*, *hoxc6a* and *hoxc8a* were shown to be specifically expressed in the anterior

portion of the primitive gut, which gives rise to swim bladder primordium (Zheng et al., 2011). Thus, the swim bladder defects in *hoxca* cluster mutants may be caused by the combined loss-of-function of these *hoxca* genes. These results suggest that *HoxC*-derived *hoxca* and *hoxcb* clusters acquire new functions to contribute to the development of teleost-specific structures in the teleost lineage. In addition, *hoxca* cluster mutants show an increased number of somites and axial vertebrae. Elongation of the posterior body has been shown to be regulated by vertebrate Hox genes (Denans et al., 2015). Our results suggest that hox genes in the *hoxca* cluster are preferentially responsible for this process in zebrafish.

In mice, deletion of the entire *HoxD* cluster results in malformations and fusions of anterior vertebrae and truncation of the limbs (Spitz et al., 2001; Zakany et al., 2001). In contrast, zebrafish *hoxda* cluster mutants did not show anterior transformation of the anteriormost vertebrae but exhibited anterior transformation in the pleural-caudal region. In addition, zebrafish *hoxda* cluster mutants did not show any malformation of pectoral fins during embryogenesis and even in adult fish. The absence of pectoral fin defects in zebrafish *hoxda* cluster mutants is not due to compensation by the *HoxD*-related *hoxdb* cluster, because zebrafish have lost the *hoxdb* cluster except for microRNA (Amores et al., 1998; Woltering and Durston, 2006). In mice, *HoxA/D* clusters redundantly function to pattern the distal forelimb (Kmita et al., 2005). In this study, we have shown that the pectoral fins in zebrafish *HoxA/D*-related *hoxaa*, *hoxab* and *hoxda* cluster mutants were not significantly affected at 3 dpf. However, the pectoral fins in individual *hoxaa* and *hoxab* cluster mutants at 5 dpf were shortened, whereas those in *hoxda* cluster mutants appeared to be normal (Fig. 3). During the early stage of pectoral fin development, *hox9-13* genes in *hoxab* and *hoxda* clusters are overlappingly expressed in the fin bud, and relatively weak expression of *hoxa9a/a11a* is confined to the fin mesenchymal cells (Ahn and Ho, 2008). After the transition of the embryonic fin buds into larval pectoral fins (48-60 hpf), the expression of posterior hox genes in the *hoxda* cluster and *hoxa9a/a11a* is gradually weakened, whereas the expression of *hoxa13a* is upregulated in the fin-fold and the expression of posterior hox genes in the *hoxab* cluster persists (Ahn and Ho, 2008). The differences of phenotypes in the pectoral fin formation in individual *hoxaa*, *hoxab* and *hoxda* cluster mutants may be caused by differential expression patterns of zebrafish *hoxaa*, *hoxab*

and *hoxda* genes. Taken together, our results suggest that the contribution of the zebrafish *hoxda* cluster to appendage formation is less than that of the mouse *HoxD* cluster and that the degree of the contribution of each Hox cluster has diversified after the quadruplication of Hox clusters.

Our study revealed phenotypic differences of homologous Hox cluster mutants between mice and zebrafish. As both are derived from common primitive vertebrates that are thought to possess quadrupled Hox clusters, our results suggest that Hox clusters in mice and zebrafish underwent discrete subfunctionalization and neofunctionalization in their respective lineages. Functional discrepancies of Hox genes between mice and zebrafish have been pointed out (Hunter and Prince, 2002; McClintock et al., 2002). In zebrafish, *hoxb1a* and *hoxb1b* play roles similar to those of mouse *Hoxa1* and *Hoxb1*, respectively, in hindbrain patterning (McClintock et al., 2001, 2002). However, zebrafish *hoxa1a*, an ortholog of mouse *Hoxa1*, is unlikely to possess such a function because segmental expression of *hoxa1a* was not detected in the hindbrain as is observed in mouse *Hoxa1* (McClintock et al., 2001). In another case, zebrafish *hoxa2b* and *hoxb2a* have a function similar to that of mouse *Hoxa2* in second pharyngeal arch formation (Hunter and Prince, 2002). In contrast, it appears that mouse *Hoxb2*, an ortholog of zebrafish *hoxb2a*, does not play a major role in this process. In this study, by analyzing the phenotypes of seven individual hox cluster mutants, we also found that responsible Hox genes are not always located in homologous Hox clusters between mice and zebrafish, suggesting that functional discrepancies of Hox genes between mice and zebrafish are widely present. Changes in *cis*-regulatory elements have been recognized as an important molecular mechanism underlying phenotypic evolution. As was previously proposed to explain the functional discrepancies of paralog 1 genes in hindbrain patterning (McClintock et al., 2001, 2002; Prince, 2002), evolutionary changes of *cis*-regulatory modules of Hox genes may occur in the teleost lineage and change the responsible Hox genes between zebrafish and mice. Alternatively, it is possible that such an event also took place in the tetrapod lineage or both lineages. We could not identify which zebrafish hox gene(s) is responsible for the specific defects observed in hox cluster mutants. Thus, deciphering the zebrafish Hox code in comparison with the mouse Hox code will provide significant insights not only into the ancestral states of Hox gene function in common primitive vertebrates but also different sub/neofunctionalization of Hox genes between zebrafish and mice.

Finally, our collection of all of the zebrafish hox cluster mutants provides valuable genetic resources not only for the elucidation of hox gene functions in zebrafish development but also for comparative studies to evaluate the evolution of vertebrate Hox genes. As functional redundancy between teleost-specific duplicated hox clusters is expected, it would be interesting to compare the phenotypes of zebrafish double mutants of these clusters with those of homologous Hox cluster mutant mice with respect to the evaluation of differential contribution of Hox genes in patterning the appendicular skeleton and the vertebral column in fish and mice in a future study.

MATERIALS AND METHODS
Zebrafish
All of the experiments were performed using Riken WT (RW) fish, which were maintained at 27°C with a 14 h light/10 h dark cycle. Embryos were obtained from natural spawning and developmental stages were determined based on the hours or days post fertilization (hpf, dpf) or the morphological features as previously described (Kimmel et al., 1995). All of the experiments using live zebrafish were approved by the Committee for Animal Care and Use of Saitama University and conducted under the regulations of Saitama University.

Zebrafish genomic information
Genomic information including the genomic structures of hox clusters is based on DNA sequences deposited in the zebrafish Ensembl database (GRCz11, release 91).

Generation of zebrafish hox cluster mutants using the CRISPR-Cas9 system
For the generation of hox cluster mutants except for the *hoxcb* cluster, the genomic region encompassing each hox cluster was deleted using the Alt-R CRISPR-Cas9 system (Integrated DNA Technologies). Briefly, two crRNAs, which are targeted to hox genes located at both ends of each cluster, were selected by using the web program CRISPR Design (http://CRISPR.mit.edu) or CHOPCHOP (http://chopchop.cbu.uib.no/index.php). The sequences of synthesized crRNAs used in this study are listed in Table S2. Target-specific crRNA was incubated with common tracrRNA to prepare the crRNA:tracrRNA duplex. Two crRNA:tracrRNA duplexes, which recognized both ends of each hox cluster, were incubated with Cas9 nuclease according to the manufacturer's protocol. Approximately 1 nl of crRNA:tracrRNA-Cas9 solution was injected into zebrafish fertilized embryos. After sexual maturation of the injected fish, candidate founder fish were mated with wild-type fish to generate hemizygous F1 offspring. F1 juvenile fish carrying the deletion of each hox cluster were identified by PCR using the genomic DNA derived from the partially dissected tailfin. Adult fish carrying hemizygous deficiency for each hox cluster are externally normal and fertile. By intercross between male and female fish possessing the same mutation, homozygous mutants were obtained. Using the genomic DNA extracted from homozygous mutant embryos, the deletion of each hox cluster was confirmed by PCR using primers specific to hox genes located within a cluster and flanking genomic regions (Table S4). As we observed translocation of the deleted hox cluster into another genomic region in some cases, the absence of the target locus was confirmed by performing PCR for hox genes in each cluster.

For generation of the *hoxcb* cluster mutant, frameshift mutations were introduced in all of the four *hoxcb* genes. Deletion of the *hoxcb* cluster by two gRNAs targeted at both ends of the *hoxcb* cluster was not accomplished due to poor efficiency. Frameshift mutations were first introduced in *hoxc11b* and *hoxc12b* using the Alt-R CRISPR-Cas9 system (Integrated DNA Technologies). Subsequently, frameshift mutations of *hoxc6b* and *hoxc13b* were introduced using the CRISPR-Cas9 system in the same allele of mutated *hoxc11b* and *hoxc12b*. The introduced mutations were confirmed by DNA sequencing.

The alleles of mutants described in this study are as follows: *hoxaa* cluster mutant, *sud111*; *hoxab* cluster mutant, *sud112*; *hoxba* cluster mutant, *sud113*; *hoxbb* cluster mutant, *sud114*; *hoxca* cluster mutant, *sud115*; *hoxcb* cluster mutant, *sud124*; and *hoxda* cluster mutant, *sud116*. Frozen sperms derived from all of the mutants have been deposited in the National BioResource Project Zebrafish in Japan (https://shigen.nig.ac.jp/zebra/).

Genotyping of hox cluster mutants
Genotyping was carried out for the maintenance of mutant fish lines or the analysis of stained embryos. Genomic DNA was extracted from live or stained embryos or dissected tailfins using the NaOH method (Meeker et al., 2007) and was used as a template for PCR-based genotyping. For six hox cluster mutants excluding *hoxcb*, three primers were used to distinguish the genotype of each mutant. For *hoxcb* cluster mutants, the genotyping was determined using primers to amplify the genomic regions surrounding the mutations in *hoxc6b*, *hoxc11b*, *hoxc12b* or *hoxc13b*, respectively. The PCR conditions and the sequences of the primers are listed in Table S3.

Whole-mount *in situ* hybridization
Whole-mount *in situ* hybridization was performed as described previously (Thisse and Thisse, 2014). Stained embryos mounted in 80% glycerol were photographed under a stereomicroscope (Leica M205 FA) with a digital

DEVELOPMENT

camera (Leica DFC350F). After taking the photos, the genotype from the stained embryos was determined by PCR as described above.

Staining of neuromast cells in the zebrafish lateral line

Neuromast hair cells in the zebrafish lateral line were stained by 4-Di-2Asp [4-(4-diethylaminostyryl)-N-methylpyridinium iodide; Sigma-Aldrich] as previously described (Sapede et al., 2002). Briefly, live larvae at 3 dpf were incubated in 100 μM of 4-Di-2Asp in 1/3 Ringer's solution for 10 min. After washing several times with 1/3 Ringer's solution, the anesthetized larvae were mounted in 2% methylcellulose and photographed under a fluorescent stereomicroscope (Leica M205 FA). Subsequently, genotyping of the stained larvae was carried out by PCR as described above. By using merged images of fluorescence and brightfield, the position of neuromasts on both sides was determined on the basis of the somite number. For neuromasts located posterior to the 30th somite, their position was regarded as >30 owing to the difficulty in distinguishing the small somites in the tail region.

Immunostaining of reticulospinal neurons

Reticulospinal neurons in hindbrain at 48 hpf were stained by anti-neurofilament RMO-44 monoclonal antibody (Thermo Fisher Scientific, 13-0500, 1:50) as previously described (Banote et al., 2016). As a secondary antibody, goat anti-mouse IgG-Alexa 488-conjugated antibody (Abcam, ab150113, 1:500) was used. Subsequently, images of flat-mounted specimens were taken using a confocal microscope (Olympus FV1000).

Alcian Blue staining of zebrafish pectoral fins and jaws

For the staining of cartilage in jaws, 5 dpf larvae were fixed with 4% paraformaldehyde in PBS and stained by acid-conditioned Alcian Blue solution as previously described (Neuhauss et al., 1996). Before the staining, the posterior body of the larvae was manually dissected, and PCR-based genotyping was carried out using extracted genomic DNA. After the staining, the surrounding tissues of the jaws were digested in 0.25% trypsin-EDTA solution. The cartilage of zebrafish pectoral fins at 5 dpf was stained by acid-free Alcian Blue solution as previously described (Walker and Kimmel, 2007). After the staining, the pectoral fins were dissected. Images were obtained under a stereomicroscope (Leica M205 FA). The lengths of the endoskeletal disc and fin-fold were measured using ImageJ software.

X-ray micro-CT analysis

Skeletal structures of zebrafish were observed using X-ray micro-CT scanning as previously described (Akama et al., 2020). Adult zebrafish were fixed with 4% paraformaldehyde in PBS at 4°C overnight and were transferred to 70% ethanol. Using an X-ray micro-CT (ScanXmate-E090S105; Comscantechno), the fixed specimens were scanned at a tube voltage peak of 85 kV and a tube current of 90 μA. For scanning of the Weberian apparatus, samples were rotated 360° in steps of 0.24-0.30°, generating 1200-1500 projection images of 992×992 pixels. These micro-CT data were reconstructed using coneCTexpress software (Comscantechno) at an isotropic resolution of 4.8-5.0 μm. For the whole scanning of a zebrafish with higher resolution, the entire body was scanned in four parts for each specimen. For each part, samples were rotated 360° in steps of 0.3°, generating 1200 projection images of 992×992 pixels. The micro-CT data of each part were reconstructed and stored as a dataset with an isotropic resolution of 10 μm. Finally, the data of four sites were combined to generate a dataset of the whole specimen. Three-dimensional image analysis was performed using OsiriX MD software (Pixmeo).

After observation of the skeletal structures, soft tissues in the specimens were analyzed using X-ray micro-CT scanning. The specimens stored in 70% ethanol were gradually hydrated in distilled water and then stained overnight with 20% Lugol's solution as previously described (Maeno et al., 2019; Metscher, 2009). For the whole scanning of a zebrafish with higher resolution, the entire body was scanned in four parts for one specimen. For each part, samples were rotated 360° in steps of 0.3°, generating 1200 projection images of 992×992 pixels. The micro-CT data of each part were reconstructed and stored as a dataset with an isotropic

resolution of 9-11 μm. Subsequently, the data of four sites were combined and three-dimensional images were constructed using OsiriX MD software (Pixmeo). Finally, movies were edited using Adobe Premiere Pro (Adobe).

Author contributions
Conceptualization: A.K.; Validation: K.Y., S.A., M.K., M.S., M.I., K. Satoh, K.A., Y.K., K. Suzuki, D.K., A.K.; Formal analysis: K.Y., A.M., M.K., M.S., M.I., A.K.; Investigation: K.Y., A.M., S.A., M.K., M.S., M.I., K. Satoh, K.A., Y.K., K. Suzuki, D.K., N.H., A.K.; Writing - original draft: A.K.; Writing - review and editing: A.K.; Project administration: A.K.; Funding acquisition: A.K.

References

Ahn, D. and Ho, R. K. (2008). Tri-phasic expression of posterior Hox genes during development of pectoral fins in zebrafish: implications for the evolution of vertebrate paired appendages. *Dev. Biol.* 322, 220-233. doi:10.1016/j.ydbio.2008.06.032

Akama, K., Ebata, K., Maeno, A., Taminato, T., Otosaka, S., Gengyo-Ando, K., Nakai, J., Yamasu, K. and Kawamura, A. (2020). Role of somite patterning in the formation of Weberian apparatus and pleural rib in zebrafish. *J. Anat.* 236, 622-629. doi:10.1111/joa.13135

Amores, A., Force, A., Yan, Y.-L., Joly, L., Amemiya, C., Fritz, A., Ho, R. K., Langeland, J., Prince, V., Wang, Y. L. et al. (1998). Zebrafish hox clusters and vertebrate genome evolution. *Science* 282, 1711-1714. doi:10.1126/science.282.5394.1711

Banote, R. K., Edling, M., Eliassen, F., Kettunen, P., Zetterberg, H. and Abramsson, A. (2016). beta-Amyloid precursor protein-b is essential for Mauthner cell development in the zebrafish in a Notch-dependent manner. *Dev. Biol.* 413, 26-38. doi:10.1016/j.ydbio.2016.03.012

Bird, N. C. and Mabee, P. M. (2003). Developmental morphology of the axial skeleton of the zebrafish, Danio rerio (Ostariophysi: Cyprinidae). *Dev. Dyn.* 228, 337-357. doi:10.1002/dvdy.10387

Breau, M. A., Wilkinson, D. G. and Xu, Q. (2013). A Hox gene controls lateral line cell migration by regulating chemokine receptor expression downstream of Wnt signaling. *Proc. Natl. Acad. Sci. USA* 110, 16892-16897. doi:10.1073/pnas.1306282110

Darbellay, F., Bochaton, C., Lopez-Delisle, L., Mascrez, B., Tschopp, P., Delpretti, S., Zakany, J. and Duboule, D. (2019). The constrained architecture of mammalian Hox gene clusters. *Proc. Natl. Acad. Sci. USA* 116, 13424-13433. doi:10.1073/pnas.1904602116

Dehal, P. and Boore, J. L. (2005). Two rounds of whole genome duplication in the ancestral vertebrate. *PLoS Biol.* 3, e314. doi:10.1371/journal.pbio.0030314

Denans, N., Iimura, T. and Pourquie, O. (2015). Hox genes control vertebrate body elongation by collinear Wnt repression. *eLife* 4, e04379. doi:10.7554/eLife.04379

Duboule, D. (2007). The rise and fall of Hox gene clusters. *Development* 134, 2549-2560. doi:10.1242/dev.001065

Economides, K. D., Zeltser, L. and Capecchi, M. R. (2003). Hoxb13 mutations cause overgrowth of caudal spinal cord and tail vertebrae. *Dev. Biol.* 256, 317-330. doi:10.1016/S0012-1606(02)00137-9

Fromental-Ramain, C., Warot, X., Lakkaraju, S., Favier, B., Haack, H., Birling, C., Dierich, A., Dolle, P. and Chambon, P. (1996). Specific and redundant functions of the paralogous Hoxa-9 and Hoxd-9 genes in forelimb and axial skeleton patterning. *Development* 122, 461-472. doi:10.1242/dev.122.2.461

Grande, T. and Young, B. (2004). The ontogeny and homology of the Weberian apparatus in the zebrafish Danio rerio (Ostariophysi: Cypriniformes). *Zool. J. Linn. Soc.* 140, 241-254. doi:10.1111/j.1096-3642.2003.00097.x

Horan, G. S., Ramirez-Solis, R., Featherstone, M. S., Wolgemuth, D. J., Bradley, A. and Behringer, R. R. (1995). Compound mutants for the paralogous hoxa-4, hoxb-4, and hoxd-4 genes show more complete homeotic transformations and a dose-dependent increase in the number of vertebrae transformed. *Genes Dev.* 9, 1667-1677. doi:10.1101/gad.9.13.1667

DEVELOPMENT

Hoshijima, K., Jurynec, M. J., Klatt Shaw, D., Jacobi, A. M., Behlke, M. A. and Grunwald, D. J. (2019). Highly efficient CRISPR-Cas9-based methods for generating deletion mutations and f0 embryos that lack gene function in Zebrafish. *Dev. Cell* 51, 645-657.e644. doi:10.1016/j.devcel.2019.10.004

Hunter, M. P. and Prince, V. E. (2002). Zebrafish hox paralogue group 2 genes function redundantly as selector genes to pattern the second pharyngeal arch. *Dev. Biol.* 247, 367-389. doi:10.1006/dbio.2002.0701

Kimmel, C. B., Ballard, W. W., Kimmel, S. R., Ullmann, B. and Schilling, T. F. (1995). Stages of embryonic development of the zebrafish. *Dev. Dyn.* 203, 253-310. doi:10.1002/aja.1002030302

Kmita, M., Tarchini, B., Zakany, J., Logan, M., Tabin, C. J. and Duboule, D. (2005). Early developmental arrest of mammalian limbs lacking HoxA/HoxD gene function. *Nature* 435, 1113-1116. doi:10.1038/nature03648

Ledent, V. (2002). Postembryonic development of the posterior lateral line in zebrafish. *Development* 129, 597-604. doi:10.1242/dev.129.3.597

Maeno, A., Kohtsuka, H., Takatani, K. and Nakano, H. (2019). Microfocus X-ray CT (microCT) Imaging of Actinia equina (Cnidaria), Harmothoe sp. (Annelida), and Xenoturbella japonica (Xenacoelomorpha). *J Vis Exp* 150, e59161. doi:10.3791/59161

McClintock, J. M., Carlson, R., Mann, D. M. and Prince, V. E. (2001). Consequences of Hox gene duplication in the vertebrates: an investigation of the zebrafish Hox paralogue group 1 genes. *Development* 128, 2471-2484. doi:10.1242/dev.128.13.2471

McClintock, J. M., Kheirbek, M. A. and Prince, V. E. (2002). Knockdown of duplicated zebrafish hoxb1 genes reveals distinct roles in hindbrain patterning and a novel mechanism of duplicate gene retention. *Development* 129, 2339-2354. doi:10.1242/dev.129.10.2339

McIntyre, D. C., Rakshit, S., Yallowitz, A. R., Loken, L., Jeannotte, L., Capecchi, M. R. and Wellik, D. M. (2007). Hox patterning of the vertebrate rib cage. *Development* 134, 2981-2989. doi:10.1242/dev.007567

Medina-Martinez, O., Bradley, A. and Ramirez-Solis, R. (2000). A large targeted deletion of Hoxb1-Hoxb9 produces a series of single-segment anterior homeotic transformations. *Dev. Biol.* 222, 71-83. doi:10.1006/dbio.2000.9683

Meeker, N. D., Hutchinson, S. A., Ho, L. and Trede, N. S. (2007). Method for isolation of PCR-ready genomic DNA from zebrafish tissues. *BioTechniques* 43, 610-612, 614. doi:10.2144/000112619

Metcalfe, W. K., Mendelson, B. and Kimmel, C. B. (1986). Segmental homologies among reticulospinal neurons in the hindbrain of the zebrafish larva. *J. Comp. Neurol.* 251, 147-159. doi:10.1002/cne.902510202

Metscher, B. D. (2009). MicroCT for developmental biology: a versatile tool for high-contrast 3D imaging at histological resolutions. *Dev. Dyn.* 238, 632-640. doi:10.1002/dvdy.21857

Miller, C. T., Maves, L. and Kimmel, C. B. (2004). moz regulates Hox expression and pharyngeal segmental identity in zebrafish. *Development* 131, 2443-2461. doi:10.1242/dev.01134

Minoux, M. and Rijli, F. M. (2010). Molecular mechanisms of cranial neural crest cell migration and patterning in craniofacial development. *Development* 137, 2605-2621. doi:10.1242/dev.040048

Minoux, M., Antonarakis, G. S., Kmita, M., Duboule, D. and Rijli, F. M. (2009). Rostral and caudal pharyngeal arches share a common neural crest ground pattern. *Development* 136, 637-645. doi:10.1242/dev.028621

Morin-Kensicki, E. M., Melancon, E. and Eisen, J. S. (2002). Segmental relationship between somites and vertebral column in zebrafish. *Development* 129, 3851-3860. doi:10.1242/dev.129.16.3851

Nakamura, T., Gehrke, A. R., Lemberg, J., Szymaszek, J. and Shubin, N. H. (2016). Digits and fin rays share common developmental histories. *Nature* 537, 225-228. doi:10.1038/nature19322

Neuhauss, S. C., Solnica-Krezel, L., Schier, A. F., Zwartkruis, F., Stemple, D. L., Malicki, J., Abdelilah, S., Stainier, D. Y. and Driever, W. (1996). Mutations affecting craniofacial development in zebrafish. *Development* 123, 357-367. doi:10.1242/dev.123.1.357

Neumann, C. J., Grandel, H., Gaffield, W., Schulte-Merker, S. and Nusslein-Volhard, C. (1999). Transient establishment of anteroposterior polarity in the zebrafish pectoral fin bud in the absence of sonic hedgehog activity. *Development* 126, 4817-4826. doi:10.1242/dev.126.21.4817

Parichy, D. M., Elizondo, M. R., Mills, M. G., Gordon, T. N. and Engeszer, R. E. (2009). Normal table of postembryonic zebrafish development: staging by externally visible anatomy of the living fish. *Dev. Dyn.* 238, 2975-3015. doi:10.1002/dvdy.22113

Prince, V. (2002). The Hox Paradox: more complex(es) than imagined. *Dev. Biol.* 249, 1-15. doi:10.1006/dbio.2002.0745

Prince, V. E., Joly, L., Ekker, M. and Ho, R. K. (1998a). Zebrafish hox genes: genomic organization and modified colinear expression patterns in the trunk. *Development* 125, 407-420. doi:10.1242/dev.125.3.407

Prince, V. E., Moens, C. B., Kimmel, C. B. and Ho, R. K. (1998b). Zebrafish hox genes: expression in the hindbrain region of wild-type and mutants of the segmentation gene, valentino. *Development* 125, 393-406. doi:10.1242/dev.125.3.393

Sanger, T. and McCune, A. (2002). Comparative osteology of the Danio (Cyprinidae: Ostariophysi) axial skeleton with comments on Danio relationships based on molecules and morphology. *Zool. J. Linn. Soc.* 135, 529-546. doi:10.1046/j.1096-3642.2002.00014.x

Sapede, D., Gompel, N., Dambly-Chaudiere, C. and Ghysen, A. (2002). Cell migration in the postembryonic development of the fish lateral line. *Development* 129, 605-615. doi:10.1242/dev.129.3.605

Sordino, P., van der Hoeven, F. and Duboule, D. (1995). Hox gene expression in teleost fins and the origin of vertebrate digits. *Nature* 375, 678-681. doi:10.1038/375678a0

Soshnikova, N., Dewaele, R., Janvier, P., Krumlauf, R. and Duboule, D. (2013). Duplications of hox gene clusters and the emergence of vertebrates. *Dev. Biol.* 378, 194-199. doi:10.1016/j.ydbio.2013.03.004

Spitz, F., Gonzalez, F., Peichel, C., Vogt, T. F., Duboule, D. and Zakany, J. (2001). Large scale transgenic and cluster deletion analysis of the HoxD complex separate an ancestral regulatory module from evolutionary innovations. *Genes Dev.* 15, 2209-2214. doi:10.1101/gad.205701

Suemori, H. and Noguchi, S. (2000). Hox C cluster genes are dispensable for overall body plan of mouse embryonic development. *Dev. Biol.* 220, 333-342. doi:10.1006/dbio.2000.9651

Thisse, B. and Thisse, C. (2014). In situ hybridization on whole-mount zebrafish embryos and young larvae. *Methods Mol. Biol.* 1211, 53-67. doi:10.1007/978-1-4939-1459-3_5

Thisse, B., Pflumio, S., Fürthauer, M., Loppin, B., Heyer, V., Degrave, A., Woehl, R., Lux, A., Steffan, T., Charbonnier, X. Q. et al. (2001). Expression of the zebrafish genome during embryogenesis. *ZFIN on-line publication*.

Trainor, P. A. and Krumlauf, R. (2000). Patterning the cranial neural crest: hindbrain segmentation and Hox gene plasticity. *Nat. Rev. Neurosci.* 1, 116-124. doi:10.1038/35039056

Trainor, P. A. and Krumlauf, R. (2001). Hox genes, neural crest cells and branchial arch patterning. *Curr. Opin. Cell Biol.* 13, 698-705. doi:10.1016/S0955-0674(00)00273-8

Vieux-Rochas, M., Mascrez, B., Krumlauf, R. and Duboule, D. (2013). Combined function of HoxA and HoxB clusters in neural crest cells. *Dev. Biol.* 382, 293-301. doi:10.1016/j.ydbio.2013.06.027

Wagner, G. P., Amemiya, C. and Ruddle, F. (2003). Hox cluster duplications and the opportunity for evolutionary novelties. *Proc. Natl. Acad. Sci. USA* 100, 14603-14606. doi:10.1073/pnas.2536656100

Walker, M. B. and Kimmel, C. B. (2007). A two-color acid-free cartilage and bone stain for zebrafish larvae. *Biotech. Histochem.* 82, 23-28. doi:10.1080/10520290701333558

Waxman, J. S., Keegan, B. R., Roberts, R. W., Poss, K. D. and Yelon, D. (2008). Hoxb5b acts downstream of retinoic acid signaling in the forelimb field to restrict heart field potential in zebrafish. *Dev. Cell* 15, 923-934. doi:10.1016/j.devcel.2008.09.009

Weicksel, S. E., Gupta, A., Zannino, D. A., Wolfe, S. A. and Sagerstrom, C. G. (2014). Targeted germ line disruptions reveal general and species-specific roles for paralog group 1 hox genes in zebrafish. *BMC Dev. Biol.* 14, 25. doi:10.1186/1471-213X-14-25

Wellik, D. M. and Capecchi, M. R. (2003). Hox10 and Hox11 genes are required to globally pattern the mammalian skeleton. *Science* 301, 363-367.

Wellik, D. M., Hawkes, P. J. and Capecchi, M. R. (2002). Hox11 paralogous genes are essential for metanephric kidney induction. *Genes Dev.* 16, 1423-1432. doi:10.1101/gad.993302

Woltering, J. M. and Durston, A. J. (2006). The zebrafish hoxDb cluster has been reduced to a single microRNA. *Nat. Genet.* 38, 601-602. doi:10.1038/ng0606-601

Ye, Z. and Kimelman, D. (2020). Hox13 genes are required for mesoderm formation and axis elongation during early zebrafish development. *Development* 147, 185298. doi:10.1242/dev.185298

Zakany, J. and Duboule, D. (2007). The role of Hox genes during vertebrate limb development. *Curr. Opin. Genet. Dev.* 17, 359-366. doi:10.1016/j.gde.2007.05.011

Zakany, J., Kmita, M., Alarcon, P., de la Pompa, J. L. and Duboule, D. (2001). Localized and transient transcription of Hox genes suggests a link between patterning and the segmentation clock. *Cell* 106, 207-217. doi:10.1016/S0092-8674(01)00436-6

Zheng, W., Wang, Z., Collins, J. E., Andrews, R. M., Stemple, D. and Gong, Z. (2011). Comparative transcriptome analyses indicate molecular homology of zebrafish swimbladder and mammalian lung. *PLoS ONE* 6, e24019. doi:10.1371/journal.pone.0024019

DEVELOPMENT